



## Research article

# The use of rapid, small-scale column tests to determine the efficiency of bauxite residue as a low-cost adsorbent in the removal of dissolved reactive phosphorus from agricultural waters

Patricia B. Cusack<sup>a, b, c</sup>, Oisín Callery<sup>d</sup>, Ronan Courtney<sup>a, c</sup>, Éva Ujaczki<sup>c, e, f</sup>, Lisa M.T. O'Donoghue<sup>f</sup>, Mark G. Healy<sup>b, \*</sup>

<sup>a</sup> Department of Biological Sciences, University of Limerick, Castletroy, Co. Limerick, Ireland

<sup>b</sup> Civil Engineering, National University of Ireland, Galway, Ireland

<sup>c</sup> The Bernal Institute, University of Limerick, Castletroy, Co. Limerick, Ireland

<sup>d</sup> Earth and Ocean Sciences, National University of Ireland, Galway, Ireland

<sup>e</sup> Department of Applied Biotechnology and Food Science, Faculty of Chemical Technology and Biotechnology, Budapest University of Technology and Economics, Műegyetem rkp. 3, 1111, Budapest, Hungary

<sup>f</sup> School of Engineering, University of Limerick, Castletroy, Co. Limerick, Ireland

## ARTICLE INFO

## Keywords:

Bauxite residue  
Adsorbent  
Phosphorus  
Agricultural wastewater

## ABSTRACT

Bauxite residue, the by-product produced in the alumina industry, is a potential low-cost adsorbent in the removal of phosphorus (P) from aqueous solution, due to its high composition of residual iron oxides such as hematite. Several studies have investigated the performance of bauxite residue in removing P; however, the majority have involved the use of laboratory “batch” tests, which may not accurately estimate its actual performance in filter systems. This study investigated the use of rapid small-scale column tests to predict the dissolved reactive phosphorus (DRP) removal capacity of bauxite residue when treating two agricultural waters of low (forest run-off) and high (dairy soiled water) phosphorus content. Bauxite residue was successful in the removal of DRP from both waters, but was more efficient in treating the forest run-off. The estimated service time of the column media, based on the largest column studied, was 1.08 min g<sup>-1</sup> media for the forest run-off and 0.28 min g<sup>-1</sup> media for the dairy soiled water, before initial breakthrough time, which was taken to be when the column effluent reached approximately 5% of the influent concentration, occurred. Metal(loid) leaching from the bauxite residue, examined using ICP-OES, indicated that aluminium and iron were the dominant metals present in the treated effluent, both of which were above the EPA parametric values (0.2 mg L<sup>-1</sup> for both Al and Fe) for drinking water.

## Nomenclature

|                                |  |
|--------------------------------|--|
| A                              | constant of proportionality (mg g <sup>-1</sup> )                          |
| a**                            | a time constant  |
| Al                             | aluminium  |
| Al <sub>2</sub> O <sub>3</sub> | aluminium oxide  |
| As                             | arsenic  |
| B                              | constant of system heterogeneity in Eqns. (1) and (2)                      |
| BRDA                           | bauxite residue disposal area  |
| Ca                             | calcium  |
| Cd                             | cadmium  |
| C <sub>t</sub>                 | solution adsorbate concentration at any filter depth (mg L <sup>-1</sup> ) |
| C <sub>0</sub>                 | influent contaminant concentration (mg L <sup>-1</sup> )                   |
| Cr                             | chromium   |

|                                |  |
|--------------------------------|--|
| CRM                            | critical raw material                                    |
| Cu                             | copper   |
| DRP                            | dissolved reactive phosphorus (mg L <sup>-1</sup> )      |
| DSW                            | dairy soiled water                                       |
| EDS                            | energy-dispersive X-ray spectroscopy                     |
| Fe                             | iron   |
| Fe <sub>2</sub> O <sub>3</sub> | iron oxide   |
| Fl                             | fluoride   |
| FT-IR                          | Fourier transform infrared                               |
| Ga                             | gallium  |
| Hg                             | mercury  |
| HNO <sub>3</sub>               | nitric acid  |
| ICP-OES                        | inductively coupled plasma optical emission spectrometer |
| M                              | mass of filter media contained in the filter column (g)  |
| Mg                             | magnesium  |
| Mn                             | manganese  |

\* Corresponding author. Alice Perry Engineering Building, College of Engineering and Informatics, National University of Ireland, Galway, Co. Galway, H91 HX31, Ireland.  
Email address: mark.healy@nuigalway.ie (M.G. Healy)

|                |  |
|----------------|--|
| Mo             | molybdenum   |
| n              | the number of containers in which the total volume of effluent is collected  |
| N              | nitrogen   |
| Na             | sodium   |
| Ni             | nickel   |
| P              | phosphorus   |
| Pb             | lead   |
| pH             | pH unit  |
| q <sub>e</sub> | cumulative mass of contaminant adsorbed per g of filter media (mg g <sup>-1</sup> )  |
| q <sub>t</sub> | time dependent sorbate concentration per unit mass of adsorbent (mg g <sup>-1</sup> ), RSSCT rapid small-scale column test |
| Se             | selenium   |
| SEM            | scanning electron microscopy   |
| t              | Empty bed contact time of the column filter bed (min)  |
| V              | volume of the influent loaded onto the filter (L)  |
| V              | vanadium   |
| V <sub>B</sub> | number of empty bed volumes of influent/solution filtered  |
| XRD            | x-ray diffraction  |
| XRF            | x-ray fluorescence   |
| Zn             | zinc   |

## 1. Introduction

Phosphorus (P) is an essential component of all plant and animal life (Weissert and Kehr, 2018), and is critical in the production and maintenance of food supply (Cordell and White, 2011; Pretty and Bharucha, 2014). Phosphorus is also identified as one of the key nutrients that leads to the eutrophication of water bodies, in which there is an excess production of algal blooms, resulting in detrimental effects to aquatic life (Pan et al., 2018). Agricultural practices, such as the application of slurry and fertiliser, may result in the transport of nutrients in surface runoff (Murnane et al., 2016; Pan et al., 2018) and subsurface flow (O' Flynn et al., 2018; Zhou et al., 2016) to

a water body, and have been identified as a major cause of eutrophication (Sharpley, 2016).

The movement of P from soil to water bodies is predominantly in the form of particulate or dissolved reactive P (DRP) (Brennan et al., 2014), the latter being 100% available for aquatic biota and which, therefore, has an immediate effect on the surrounding ecosystems (Penn et al., 2014). Conventional methods of P removal from water have involved the use of enhanced biological removal systems such as polyphosphate accumulating organisms (PAOs) (Ge et al., 2015) and algal biofilms (Sukačová et al., 2015), precipitation methods using hydrous ferric oxides (Hauduc et al., 2015) or struvite (Zhou et al., 2015), the use of adsorbents (Grace et al., 2015; Callery et al., 2016; Callery and Healy, 2017), ion exchange (Acelas et al., 2015), and reverse osmosis (Wang et al., 2016). In recent years, to address the concept of a 'circular economy' (United Nations, 2015), emphasis has been placed on the utilisation of industrial wastes as low-cost adsorbents (De Gisi et al., 2016; Grace et al., 2016). Materials that have been utilised include fly ash (Nowak et al., 2013), steel slags (Claveau-Mallet et al., 2013) and chemical amendments (Callery et al., 2015). Particular focus has been placed on bauxite residue (red mud), the by-product generated in the Bayer Process during the extraction of alumina, as a potential low-cost P adsorbent in aqueous solutions. It is currently being produced at a global rate of 150 Mt per annum (Evans, 2016), but only approximately 2% of the bauxite residue produced is currently re-used (Ujaczki et al., 2018), with the remaining ~98% being disposed of into bauxite residue disposal areas (BRDAs) (Burke et al., 2013; Kong et al., 2017). The general composition of bauxite residue comprises high amounts of iron (Fe) and aluminium (Al) oxides (Zhu et al., 2016), which are good adsorbents of P. In addition, bauxite residue has a high specific surface area (Gräfe et al., 2011) and therefore has numerous potential adsorption sites, giving it increased capacity for P retention. Previous laboratory studies have shown that bauxite residue has high P adsorption capacity (Table 1).

Traditionally, bench-scale "batch" studies are conducted to evaluate the effectiveness of a material to adsorb P (Table 1). These studies involve placing the material in small containers, overlaying it with solutions of known concentrations, mixing for a period usually of between 24 and 48 h, and then fitting the results obtained to an adsorption isotherm such as the Freundlich

**Table 1**  
Phosphorus (P) adsorption studies that have been carried out using bauxite residue, untreated and treated residues, and their recovery efficiencies (adapted from Cusack et al., 2018).

|  | P recovery technique        | Factors investigated                     | Type of water              | Initial P concentration of the water | P recovered                    | Reference              |
|--|-----------------------------|--|----------------------------|--------------------------------------|--------------------------------|------------------------|
| Untreated bauxite residue  | Batch adsorption experiment | Kinetics, pH and temperature             | Synthetic water            | 5–100 mg P L <sup>-1</sup>           | 0.20 mg P g <sup>-1</sup>      | Grace et al. (2015)    |
| Untreated bauxite residue  | Column study                | Initial concentration, particle size     | Synthetic water            | 60–1000 mg P L <sup>-1</sup>         | 25 mg P g <sup>-1a</sup>       | Herron et al., 2016    |
| Untreated bauxite residue  | Batch adsorption experiment | Initial concentration, pH, particle size | Synthetic water            | 10–150 mg P L <sup>-1</sup>          | 0.345–1 mg P g <sup>-1</sup>   | Cusack et al. (2018)   |
| Gypsum Treated   | Batch adsorption experiment | Contact time                             | Synthetic water            | 20–400 mg P L <sup>-1</sup>          | 7.03 mg P g <sup>-1</sup>      | Lopez et al. (1998)    |
| Gypsum Treated   | Batch adsorption experiment | Initial concentration, pH, particle size | Synthetic water            | 10–150 mg P L <sup>-1</sup>          | 1.39–2.73 mg P g <sup>-1</sup> | Cusack et al. (2018)   |
| Seawater Treated   | Batch adsorption experiment | Initial concentration, pH, particle size | Synthetic water            | 10–150 mg P L <sup>-1</sup>          | 0.48–1.92 mg P g <sup>-1</sup> | Cusack et al. (2018)   |
| Brine treated bauxite residue (Bauxsol <sup>TMb</sup> )          | Batch adsorption experiment | pH, ionic strength, time                 | Synthetic water            | 0.5–2 mg P L <sup>-1</sup>           | 6.5–14.9 mg P g <sup>-1</sup>  | Akhurst et al. (2006)  |
| Brine treated bauxite residue (Bauxsol <sup>TMb</sup> )          | Column study                | Kinetics, particle size                  | Secondary treated effluent | 3–9.2 mg P L <sup>-1</sup>           | 2.85–8.74 mg P g <sup>-1</sup> | Despland et al. (2011) |
| Acid and brine treated bauxite residue (Bauxsol <sup>TMb</sup> ) | Batch adsorption experiment | Kinetics and isotherms                   | Synthetic water            | 200 mg P L <sup>-1</sup>             | 55.72 mg P g <sup>-1</sup>     | Ye et al. (2014)       |
| Heat treated bauxite residue                                     | Batch adsorption experiment | Time, pH and initial concentration       | Synthetic water            | 155 mg P L <sup>-1</sup>             | 155.2 mg P g <sup>-1</sup>     | Liu et al. (2007)      |
| Acid and heat treated bauxite residue                            | Batch adsorption experiment | Time, pH and initial concentration       | Synthetic water            | 155 mg P L <sup>-1</sup>             | 202.9 mg P g <sup>-1</sup>     | Liu et al. (2007)      |
| Acid treated bauxite residue                                     | Batch adsorption experiment | Acid type, pH                            | Synthetic water            | 1 mg P L <sup>-1</sup>               | 1.1 mg P g <sup>-1</sup>       | Huang et al. (2008)    |

<sup>a</sup> P<sub>max</sub> value given i.e. Maximum amount of P adsorbed per g of media, as determined using the Langmuir adsorption isotherm.

<sup>b</sup> Bauxsol<sup>TM</sup> = neutralised bauxite residue produced using the Basecon<sup>TM</sup> procedure, which uses brines high in Ca<sup>2+</sup> and Mg<sup>2+</sup> (McConchie et al., 2001).

or Langmuir, in order to quantify its adsorption potential (Cusack et al., 2018; Grace et al., 2015). However, batch studies have some disadvantages, such as failing to replicate the often passive nature of the adsorption process which exists on site, as well as sometimes using unrealistic ratios of adsorbent to solution, and shaking of the samples (Ádám et al., 2007; Søvik and Kløve, 2005). In addition, concerns have been raised about their accuracy in replicating the actual performance when the adsorbent material is placed in a filter and operated on site (Fenton et al., 2009). Due to the nature of the batch experiment, they also fail to realistically replicate any incidental releases of contaminants, which may occur when some materials are placed in filters. This may be particularly pertinent in the evaluation of the feasibility of bauxite residue, which contains metals (Cusack et al., 2018). In order to determine the full potential and longevity of an adsorbent, larger scale “column” studies are necessary (Pratt et al., 2012). In these studies, the material is placed in a column, usually operated at laboratory-scale, and water of a known concentration is passed through the material until the effluent concentration is the same as the influent concentration. These continuous flow column studies require vast amounts of influent water, which depending on the type of water utilised, is often difficult to source in the laboratory (Callery and Healy, 2017). On account of this, rapid, small-scale column studies which utilise smaller volumes of media and wastewater have been gaining in popularity, and have been used to successfully model the adsorbencies of P (Callery et al., 2016; Lalley et al., 2015), fluoride (Wu et al., 2018), paracetamol (García-Mateos et al., 2015), and varying species of arsenic (Tresintsi et al., 2014).

As P adsorption tests on bauxite residues have been commonly conducted using batch-scale studies, which may have many shortcomings as detailed above, the objectives of this study were to use rapid, small-scale column studies to (1) to assess the potential of bauxite residue as a low-cost adsorbent for DRP removal from two types of agricultural waters (dairy soiled water (DSW) and forest run-off) (2) compare the composition of the bauxite residue before and after use in the column tests (3) investigate the speciation of P adsorption onto the bauxite residue, and (4) identify any potential trace metal mobilisation from the bauxite residue during the study.

## 2. Materials and methods

### 2.1. Sample collection

Bauxite residue was obtained from a European refinery. Residue was sampled to a depth of 30 cm below the surface of the BRDA, returned to the laboratory and dried at 105 °C for 24 h. Once dry, the samples were pulverised using a mortar and pestle and sieved to a particle size <0.5 mm. The pH and electrical conductivity (EC) were measured (n = 3) using 5 g of sample in an aqueous extract, using a 1:5 ratio (solid:liquid) (Courtney and Harrington, 2010). Dairy soiled water (milk parlour washings composed of cow faeces and urine, milk and detergents; Minogue et al., 2015) was collected from Teagasc Agricultural Research Centre, Moorepark, Co. Cork, Ireland [52° 9' 48.114" N, 8° 15' 34.6464" W] and forest run-off was collected from Kilmoon, Co. Clare, Ireland [53° 2' 48.0372" N, 9° 16' 21.1368" W]. The DSW and forest run-off were transferred directly to a temperature-controlled room (11 °C) prior to commencement of testing. The DRP was measured using filtered (0.45 µm) subsamples using a nutrient analyser (Konelab20, Thermo Clinical Lab systems, Finland) and the pH was measured using a Eutech Instruments pH 700 (Thermo Scientific, USA).

#### 2.1.1. Media characterisation

The bauxite residue was characterised before and after the experiment. Mineralogical detection was carried out on 1 g powdered samples using X-ray diffraction (XRD) on a Philips X'Pert PRO MPD® (California, USA) at 40 kV, 40 mA, 25 °C by Cu X-ray tube (K $\alpha$ -radiation). The patterns were collected in the angular range from 5 to 80° (2 $\theta$ ) with a step-size of 0.008° (2 $\theta$ ) (Castaldi et al., 2011). The surface morphology and elemental detection were

carried out using scanning electron microscopy (SEM) and energy-dispersive X-ray spectroscopy (EDS) on a Hitachi SU-70 (Berkshire, UK). X-ray fluorescence (XRF) analysis was carried out onsite at the refinery using a Panalytical Axios XRF.

### 2.2. Rapid small scale column study

Small bore adsorption columns were prepared after Callery et al. (2016) using polycarbonate tubes, with an internal diameter of 0.94 cm and lengths of 20, 30 and 40 cm. The tubes were packed with a mixture of bauxite residue. The bauxite residue was held in place within each column using acid-washed glass wool and plastic syringes with an internal diameter equal to outside diameter of the polycarbonate tube, placed at the top and bottom of each of the polycarbonate tube columns. To each end of the polycarbonate tube column, flexible silicone tubing was attached to the syringe ends in order to provide lines for the influent and effluent. The columns were secured on a metal frame, allowing for a stable, vertical orientation to be maintained. A Masterflex® L/S Variable-Speed Drive peristaltic pump (Gelsenkirchen, Germany) with a variable speed motor was used to pump the influent, DSW and forest run-off, into the base of each column at an estimated flow rate of 30.49 ± 0.85 mL h<sup>-1</sup> (equivalent to a hydraulic loading rate used in a P removal system for wastewater treatment on a poultry farm; Penn et al., 2014). The pump was operated in 12 h on/off cycles (to allow the filter media to replenish some of its adsorption sites) to achieve loading periods of 24–36 h, in order to obtain enough data points for the determination of the adsorption model coefficients. Every 2 h, aliquots of the filtered effluent were collected using an auto-sampler and measured for volume, pH and DRP.

The adsorption performance of the media was evaluated using a model developed by Callery and Healy (2017), wherein the column effluent (C<sub>e</sub>) is taken as a function of the volume of influent treated (V) and breakthrough concentrations (BTCs) formed by plotting V (x-axis) against C<sub>e</sub> (y-axis). The breakthrough of the column media was taken to be when the column effluent was approximately 5% of the influent concentration (Chen et al., 2003). This model, which has been successful in the prediction of the performance of a large-scale filter (Callery et al., 2016), was used in the prediction of the longevity of the bauxite residue in the current study.

The overall bauxite residue service time or longevity of the bauxite residue media can be found by first determining the volume treated, using Eqn. (1), where q<sub>t</sub> is the time dependent sorbate concentration per unit mass of adsorbent (mg g<sup>-1</sup>), M is the mass of the adsorbent (g), B is a constant of system heterogeneity, C<sub>o</sub> is the sorbate concentration of the influent (mg L<sup>-1</sup>) and C<sub>t</sub> is the solution adsorbate concentration at any filter depth (mg L<sup>-1</sup>), by dividing the volume treated, V (in L) by the loading rate (L s<sup>-1</sup>) and then converting to minutes per g of media.

$$V = \frac{q_t M}{B (C_o - C_t)} \quad (1)$$

The q<sub>t</sub> used in Eqn. (1) was calculated using Eqn. (2):

$$q_t = AV_B \left( \frac{1}{B} \right) \left| \frac{t}{t + a^{**}} \right| \quad (2)$$

where A is a constant of proportionality (mg L<sup>-1</sup>), t is the empty bed contact time of the column filter bed (min), V<sub>B</sub> is the number of empty bed volumes of influent/solution filtered, and a<sup>\*\*</sup> is a time constant.

### 2.3. Speciation of P adsorbed

Fourier transform infrared (FT-IR) analysis was carried out using a PerkinElmer Spectrum 100 (PerkinElmer, USA). The FT-IR spectra were recorded in the 4000 to 650 cm<sup>-1</sup> range and were collected after 256 scans at 4 cm<sup>-1</sup> resolution (Castaldi et al., 2010).

## 2.4. Trace metal analysis

Every 2 h, 10 mL of the aliquot collected from the columns, was preserved in nitric acid ( $\text{HNO}_3$ ), to a pH < 2 and refrigerated before elemental analysis was carried out using an Agilent Technologies 5100 Inductively Coupled Plasma Optical Emission Spectrometer (ICP-OES). In order to carry out the ICP-OES analysis, a calibration curve was created using standardised solutions comprised of 100, 50, 10, 5 and  $1 \text{ g L}^{-1}$  multi element standard (Inorganic Ventures, Ireland) and 1M  $\text{HNO}_3$ . The analytical lines (in nm) used for the calculations of each element were as follows: Al 237.312, 396.152; calcium (Ca) 396.847, 422.673; cadmium (Cd) 214.439, 226.502, 228.802; chromium (Cr) 205.560, 267.716, 357.868; copper (Cu) 213.598, 324.754, 327.395; Fe 234.350, 238.204, 259.940; gallium (Ga) 287.423, 294.363, 417.204; mercury (Hg) 184.887, 194.164; magnesium (Mg) 279.553, 280.270, 285.213; manganese (Mn) 257.610, 259.372, 260.568; molybdenum (Mo) 202.032, 203.846, 204.598; sodium (Na) 589.592; nickel (Ni) 216.555, 221.648, 231.604; lead (Pb) 220.353, 283.305; selenium (Se) 196.026, 203.985; silicon (Si) 250.690, 251.611, 288.158; vanadium (V) 268.796, 292.401, 309.310; zinc (Zn) 202.548, 206.200, 213.857 (Bridger and Knowles, 2000). The XRF analysis performed on the bauxite residue was carried out using a Panalytical Axios XRF (Malvern Panalytical Ltd., United Kingdom).

**Table 2**  
Main mineralogical composition (%) of the bauxite residue determined by XRF.

| Mineral oxide                           | %               |
|---|-----------------|
| Aluminum oxide, $\text{Al}_2\text{O}_3$ | $14.8 \pm 1.5$  |
| Iron oxide, $\text{Fe}_2\text{O}_3$     | $47.5 \pm 2.0$  |
| Titanium oxide, $\text{TiO}_2$          | $10.3 \pm 0.95$ |
| Silicon oxide, $\text{SiO}_2$           | $7.20 \pm 1.0$  |
| Calcium oxide, $\text{CaO}$             | $6.1 \pm 1.0$   |

## 3. Results and discussion

### 3.1. Media characterisation before and after the experiments

Bauxite residue typically comprises Fe, Al, Ti, Si, Na and Ca, mainly in the form of oxides (Gräfe et al., 2011). The presence of Fe and Al oxides, which can range from 5 to 60 and 5–30%, respectively (Evans, 2016), and Ti oxides, which are typically in the range of 0.3–15% (Evans, 2016), mean that bauxite residue is a potential adsorbent for both cations and anions from aqueous solutions (Bhatnagar et al., 2011; Cusack et al., 2018). This is why numerous studies have investigated the potential of P removal from aqueous solution (Table 1).

The main mineralogical composition of the bauxite residue used in this study comprised mainly iron and aluminium oxides ( $\text{Fe}_2\text{O}_3$  and  $\text{Al}_2\text{O}_3$ ) (Table 2). SEM-EDS analysis also indicated the dominance of Fe and Al (Fig. S1 in the Supplementary Information). Titanium, Si, Ca and Na were also detected in the main composition. Prior to use in the column, there was a mineralogical dominance of the iron oxide hematite (as represented by H in Fig. 1), detected at positions  $33.153$  and  $35.612^\circ 2\theta$ , respectively (Fig. 1). Rutile ( $\text{TiO}_2$ ) was also detected at position  $27.459^\circ 2\theta$ . Following the column trials, XRD analysis was carried out on the spent media from both the DSW and forest run-off columns. New peaks were identified in the XRD patterns, as seen in Fig. 1, which show the presence of P-based minerals, which were not present in the raw media. The new peaks detected in both the spent media following treatment of the DSW and forest run-off was calcium hydrogenphosphate (III) hydrate ( $\text{CaHPO}_4 \cdot 3\text{H}_2\text{O}$ ) at positions  $19.120$  and  $30.001^\circ 2\theta$ . The presence of this mineral in the spent media indicates P retention within the bauxite residue after treatment. The particle size analysis (PSA) of the bauxite residue used in this study is shown in Table 3.

### 3.2. Influent and effluent water characterisation and rapid small-scale column study

The forest run-off had a pH of 7.57 and a DRP concentration of  $1.10 \text{ mg P L}^{-1}$ . The total phosphorus (TP) concentration of forest run-off is usually

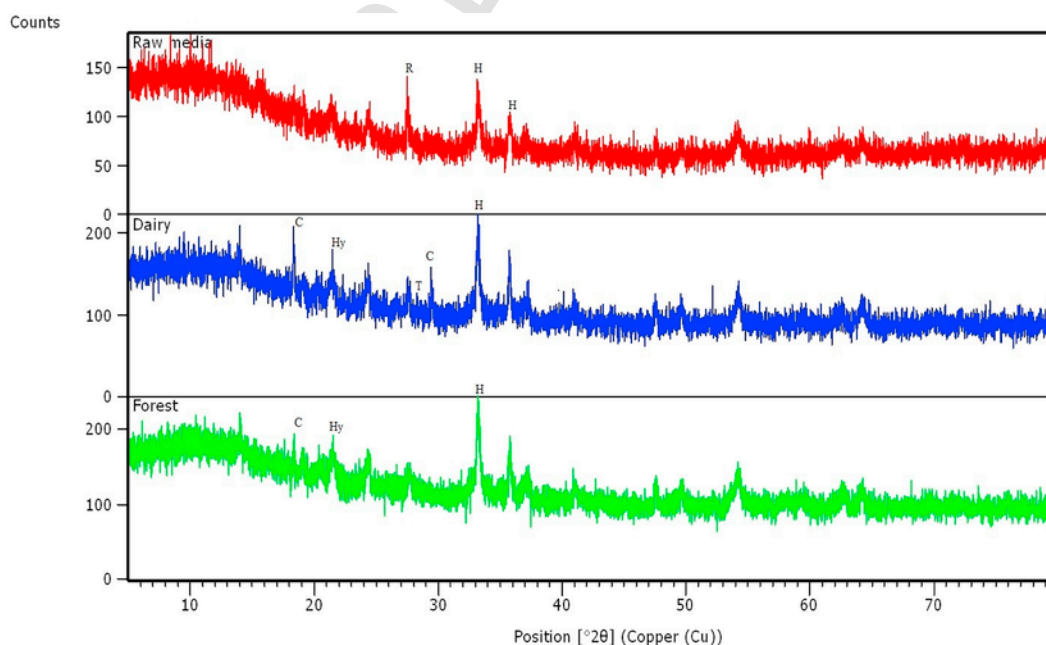


**Fig. 1.** XRD pattern as determined for the column media before ('Raw media', top) and after the loading period with DSW ('Dairy', middle) and forest run-off ('Forest', bottom). Hematite (H;  $\text{Fe}_2\text{O}_3$ ), detected at position  $33.153$  and  $35.612^\circ 2\theta$  and rutile (R;  $\text{TiO}_2$ ), detected at position  $27.459^\circ 2\theta$  were present in the raw bauxite residue media. Calcium hydrogenphosphate (III) hydrate (C;  $\text{CaHPO}_4 \cdot 3\text{H}_2\text{O}$ ), detected at positions  $19.120$  and  $30.001^\circ 2\theta$ , was present in both the spent media following treatment of the DSW and forest run-off.

**Table 3**  
Particle size distribution of the bauxite residue used in this study.

| $d_{10}$ ( $\mu\text{m}$ ) <sup>a</sup> | $d_{50}$ ( $\mu\text{m}$ ) <sup>b</sup> | $d_{90}$ ( $\mu\text{m}$ ) <sup>c</sup> |
|---|---|---|
| $0.8 \pm 0.1$                           | $2.6 \pm 0.1$                           | $6.8 \pm 0.2$                           |

<sup>a</sup>  $d_{10}$  ( $\mu\text{m}$ ) = the size of particles at 10% of the total particle distribution.  
<sup>b</sup>  $d_{50}$  ( $\mu\text{m}$ ) = the median; the size of particles at 50% of the total particle distribution.  
<sup>c</sup>  $d_{90}$  ( $\mu\text{m}$ ) = the size of particles at 90% of the total particle distribution.

around  $1 \text{ mg L}^{-1}$  (Finnegan et al., 2012), whereas DSW has a TP concentration of  $20\text{--}100 \text{ mg L}^{-1}$  and a total nitrogen (TN) concentration of  $70\text{--}500 \text{ mg L}^{-1}$  (Minogue et al., 2015). The DSW used in this study had a pH of 7.79 and a DRP concentration of  $10.64 \text{ mg P L}^{-1}$ .

The BTC approached saturation much quicker for the DSW than for the forest run-off water (Fig. 2). Similar to the findings of Vuković et al. (2011), the breakthrough time and exhaustion time increased with bed depth. As a result of its composition, there are other anions such as nitrates ( $\text{NO}_3^-$ ) and nitrites ( $\text{NO}_2^-$ ) present in the DSW (Ruane et al., 2011), and therefore there is greater competitiveness for available adsorption sites and interferences between the adsorbent surface and the ions present in the aqueous solution. This may explain why the DSW-treating columns generated a BTC approaching saturation much faster than the bauxite residue columns treating forest run-off. When treating the forest run-off, the bauxite residue had a service time of approximately 22.80 min, based on the largest column before the initial breakthrough time of the bauxite residue occurred. However, when treating the DSW, it had a shorter service time of 5.80 min, as noted for the largest column before the initial breakthrough occurred. Taking into account the amount of bauxite residue used in the largest columns (21.16 and 20.78 g), this gives an estimated service time of  $1.08 \text{ min g}^{-1}$  bauxite residue

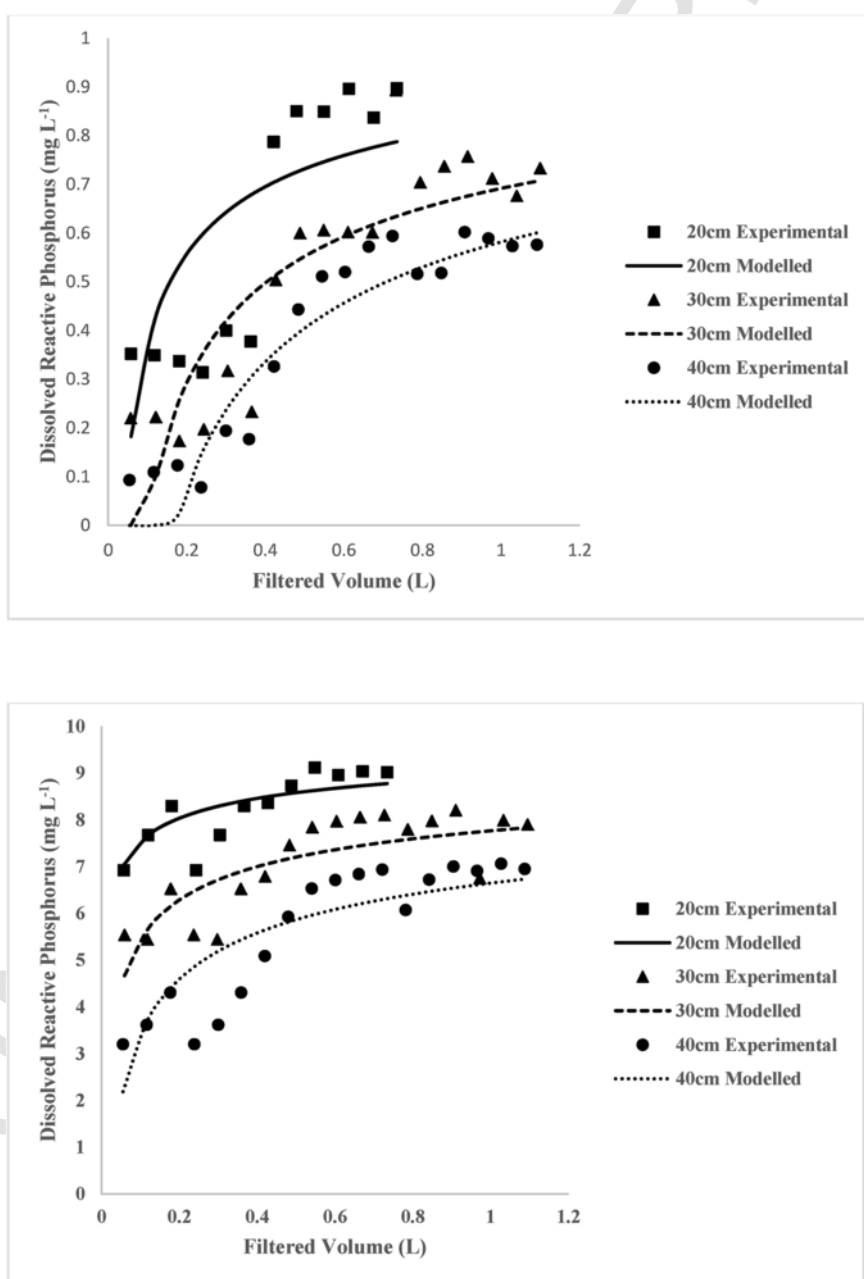


**Fig. 2.** The breakthrough curves for the effluent dissolved reactive phosphorus concentration versus loading time for forest run-off (top) and dairy soiled water (bottom) using experimental and modelled data.

and  $0.28 \text{ mg g}^{-1}$  bauxite residue when treating forest run-off and DSW, respectively, before initial breakthrough (5%) would occur.

The modelled  $q_t$  values were  $0.27 \text{ mg P g}^{-1}$  media and  $0.045 \text{ mg P g}^{-1}$  media when treating the DSW and forest run-off, respectively. These were lower than  $q_t$  values of between  $2.85$  and  $8.74 \text{ mg P g}^{-1}$  for neutralised bauxite residue (Bauxol) used to treat secondary-treated wastewater (Despland et al., 2011) and  $25 \text{ mg P g}^{-1}$  for untreated bauxite residue used to treat synthetic water (Herron et al., 2016) (Table 1). Compared to other studies that have used low-cost adsorbents such as zeolite ( $0.01 \text{ mg P g}^{-1}$  - Grace et al., 2015) and granular ceramics ( $0.9 \text{ mg P g}^{-1}$  - Chen et al., 2012), the bauxite residue in the current study had a higher P adsorbency, but it was lower than crushed concrete ( $19.6 \text{ mg P g}^{-1}$  - Egemose et al., 2012) and untreated biochar ( $32 \text{ mg P g}^{-1}$  - Wang et al., 2015). It is important to note that full saturation of the bauxite residue was not reached in the current study and the wastewaters treated may have had an impact on the P adsorption capacity, as there may have been interferences and competition for adsorption sites due to the presence of other ions and contaminants in addition to the phosphate ions.

### 3.3. Speciation of P adsorbed

The adsorption of phosphate ions onto an adsorbent is measured by the decrease for phosphate in the influent after a certain amount of time (Loganathan et al., 2014). Typically, the main mechanism of phosphate adsorption (and other anions and cations) onto the surface of iron and aluminium oxides may be separated into two processes: specific and non-specific adsorption (Stumm, 1992; Cornell and Schwertmann, 2003). Specific adsorption takes place through the process of ligand exchange (Jacukowicz-Sobala et al., 2015). A phosphate ion exchanges with one or more hydroxyl groups, with the release of  $\text{OH}_2$  and/or  $\text{OH}^-$  back into the surrounding solution, contributing to the alkalisation of the surrounding environment (Cornell and Schwertmann, 2003), as shown in the following equations:



Non-specific adsorption, which was the main mechanism evident in this study, is inclusive of electrostatic interactions and surface precipitation (Loganathan et al., 2014) between the surface of the sorbent and the phosphate ion (Jacukowicz-Sobala et al., 2015). The electrostatic interactions occur

between the electric charge carried on the surface of the sorbent and type of ion present in the surrounding solution. Phosphate ions, which are of anionic nature, carry a negative charge, which interacts with the positive charge as carried by Ca, a cation (Loganathan et al., 2014). Surface precipitation involves the formation of complexes/precipitates on the surface of the sorbent such as  $\text{CaHPO}_4^{3-}$  as a result of these ion interactions (Loganathan et al., 2014). The adsorption of the phosphate ions is greatest in a low pH environment due to the abundance of positively charged sites (Jacukowicz-Sobala et al., 2015).

X-ray diffraction and SEM analysis have been used in previous studies to show evidence of the presence of newly formed surface precipitates following the P adsorption process (Bowden et al., 2009). The XRD data obtained in this study (Fig. 1) show that the main interactions and complexes formed by the phosphate ions present in the wastewater (negative charge) were with Ca (positive charge) present in the bauxite residue, as evidenced by the presence of new peaks of  $\text{CaHPO}_4^{3-}$  in the XRD patterns following the treatment of both the DSW and forest run-off. Depending on the pH of the solution, the species of P found in aqueous solution are  $\text{H}_3\text{PO}_4$  (pH < 4),  $\text{H}_2\text{PO}_4^-$  (pH ~ 0–9),  $\text{HPO}_4^{2-}$  (pH ~ 5–11) and  $\text{PO}_4^{3-}$  (pH > 10) (Karageorgiou et al., 2007; Despland et al., 2011).

The FT-IR analysis of the bauxite residue media before and after treatment of both the DSW and forest run-off (Figs. 3 and 4) indicated that similar changes occurred in the media following treatment of both wastewaters. Two distinct broad bands were detected between wavelength  $600$  to  $900 \text{ cm}^{-1}$  and again at  $1000$  to  $1400 \text{ cm}^{-1}$ . This was evident for both the DSW and forest run-off spent media. Intensive IR absorption bands are typically in the range of  $560$ – $600 \text{ cm}^{-1}$  and  $1000$  to  $1100 \text{ cm}^{-1}$  for P species (Tejedor-Tejedor and Anderson, 1990; Berzina-Cimdina and Borodajenko, 2012). However, it was not possible to identify specific P species due to some interferences, which are most likely due to the presence of many other ions present in each of the wastewater sources used.

There was an increase in the pH in the effluent for both the DSW and forest run-off treated wastewater (Fig. 5). The influent pH of the DSW was  $7.79$ , which increased to  $8.94$  in the  $40 \text{ cm}$  column at  $t = 2 \text{ h}$ . The influent pH of the forest run-off was  $7.57$  and increased to  $8.81$  at  $t = 12 \text{ h}$  in the  $40 \text{ cm}$  column. According to the Drinking Water Directive (98/83/EC), the pH value should be in the range of  $\geq 6.5$  and  $\leq 9.5$ . The values recorded in this study show that the pH values in the effluent are within this range, highlighting no potential risk to the surrounding environment.

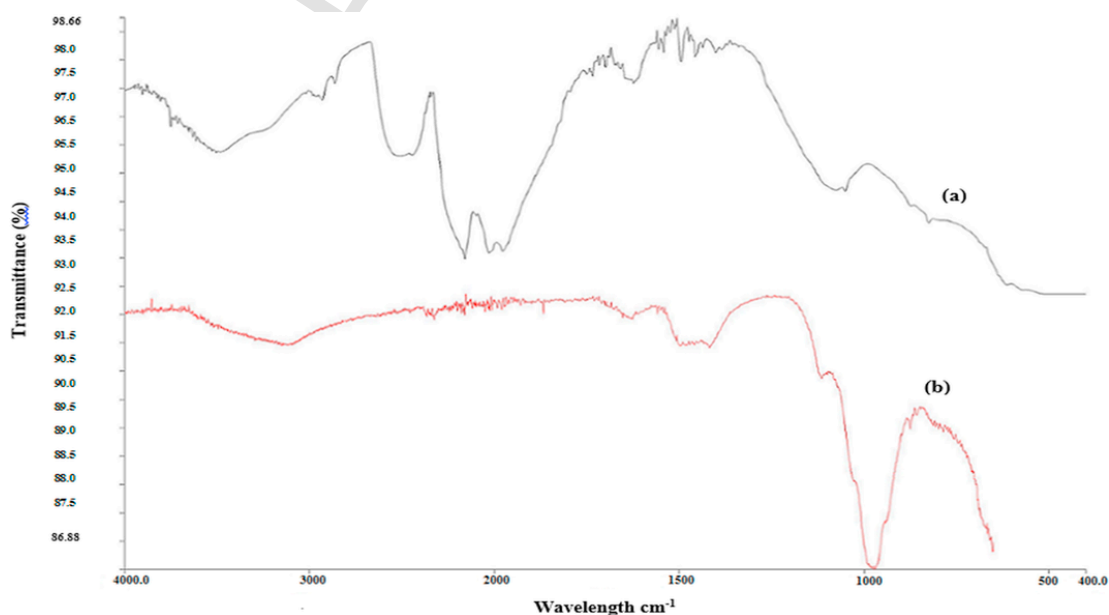


Fig. 3. FT-IR analysis of the bauxite residue media before (a) and after use in the column treating DSW (b).

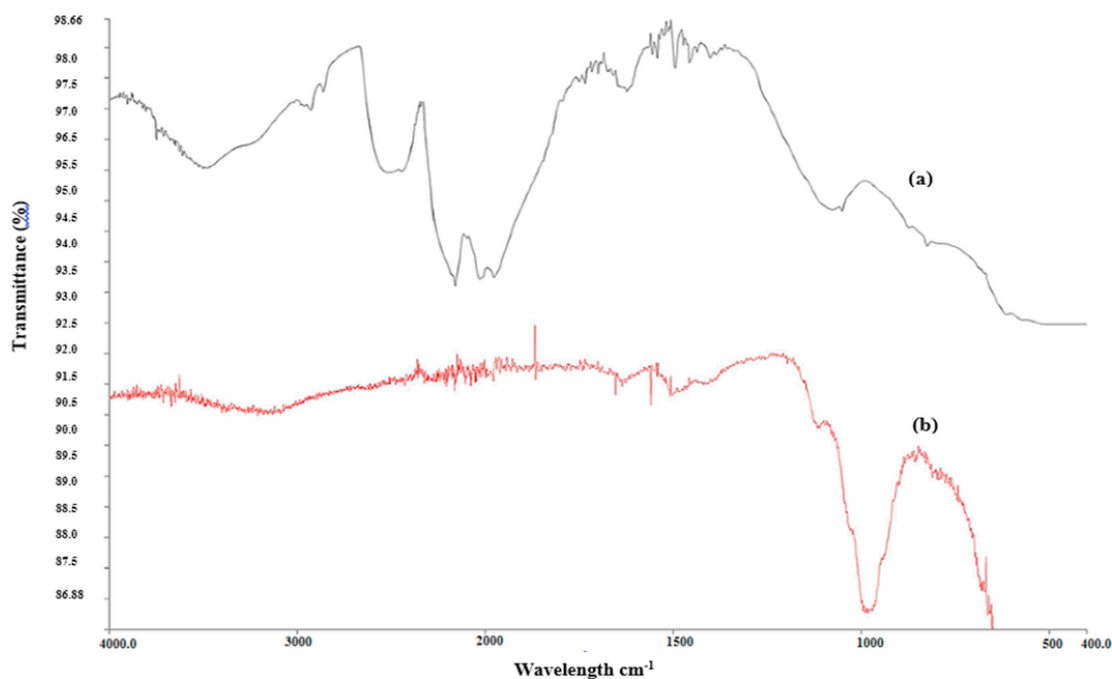


Fig. 4. FT-IR analysis of the bauxite residue media before (a) and after use in the column treating forest run-off (b).

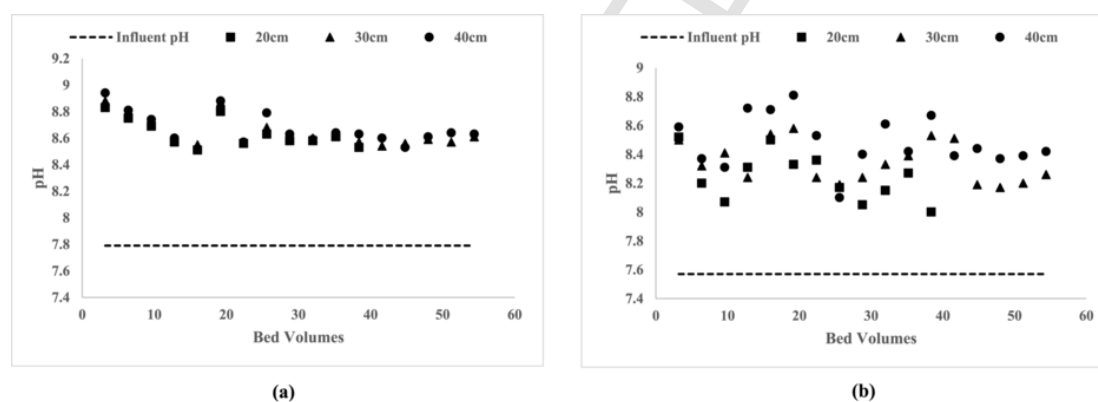


Fig. 5. The pH values of (a) the dairy soiled water and (b) forest run-off effluent from the columns over the 24–36 h loading period, showing that there was an overall increase in the pH of the effluent treated.

### 3.4. Trace metal and elemental analysis

Due to the complex nature of bauxite residue and its composition, there is potential for trace metal leaching to the surrounding environment (Despland et al., 2011; Evans, 2016). Pollution from metals can have an adverse and detrimental effect on the surrounding environment, affecting plant and animal life (Gomes et al., 2016a; Olszewska et al., 2017). In addition, the majority of metals that are in a soil environment are non-degradable (Guo et al., 2006).

The influent and effluent metal concentrations from the columns treating DSW and forest run-off, along with the parametric values, as mandated by the Irish EPA (2014), are displayed in Figs. 6 and 7. In this study, the dominant species present in both effluents were Al and Fe, which were above the parametric values ( $0.2\text{mgL}^{-1}$  for both Al and Fe). Copper was released in both effluents, but did decrease with loading time when treating the DSW and the level of Cu reduced to below the parametric value of  $2\text{mgL}^{-1}$ . The level of Mn was lower in the effluent compared to the influent for all columns, showing a retention capacity within the column media, but it was higher than the parametric value of  $0.05\text{mgL}^{-1}$ . Magnesium, Ga, V and Zn

were also present in increased amounts in the effluent, due to leaching from the bauxite residue. However, the Mg and Zn did decrease with increasing loading time. There are currently no parametric values or EPA guideline values for drinking water parameters for Mg, Ga, V and Zn, although previous studies have highlighted that bauxite residue is inclusive of oxyanionic-forming elements, which are soluble at high pH range; these include Al, As, Cr, Mo and V (Mayes et al., 2016). The main species of V present in bauxite residue was in the pentavalent form (Burke et al., 2012, 2013), which may be problematic due to its toxicity (Burke et al., 2012). Whilst V may be a potential issue (depending on the source of bauxite ore), it is also the focus of critical raw material (CRM) recovery studies (Gomes et al., 2016b; Zhu et al., 2018), which suggests the potential and need for further studies investigating the adsorbent potential of bauxite residue following the removal and recovery of CRMs such as V.

Previous work by Lopez et al. (1998) highlighted the ability of bauxite residue to retain Ni, Cu and Zn. Despland et al. (2014) showed that Bauxsol™ (neutralised bauxite residue produced using the Basecon™ procedure) had the ability to remove trace amounts of As, lead (Pb), Cd, Cr, Cu, Ni, Se, Zn, Mn and Al. This highlights the potential of bauxite residue in the removal of both cations and anions from aqueous solution. However, the com-

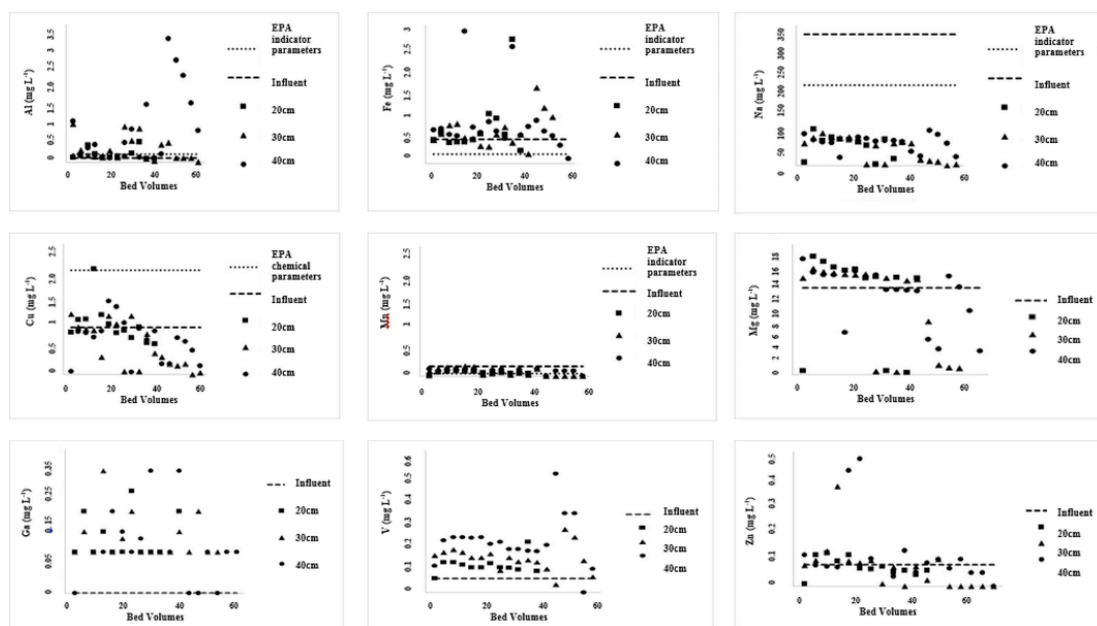


Fig. 6. Comparison of the composition of (a) Al, (b) Fe, (c) Na (d) Cu (e) Mn (f) Mg (g) Ga (h) V and (i) Zn in both the influent and effluent in the columns treating DSW over the 24–36h loading period. EPA indicator parameter or EPA chemical parameter included for each element.

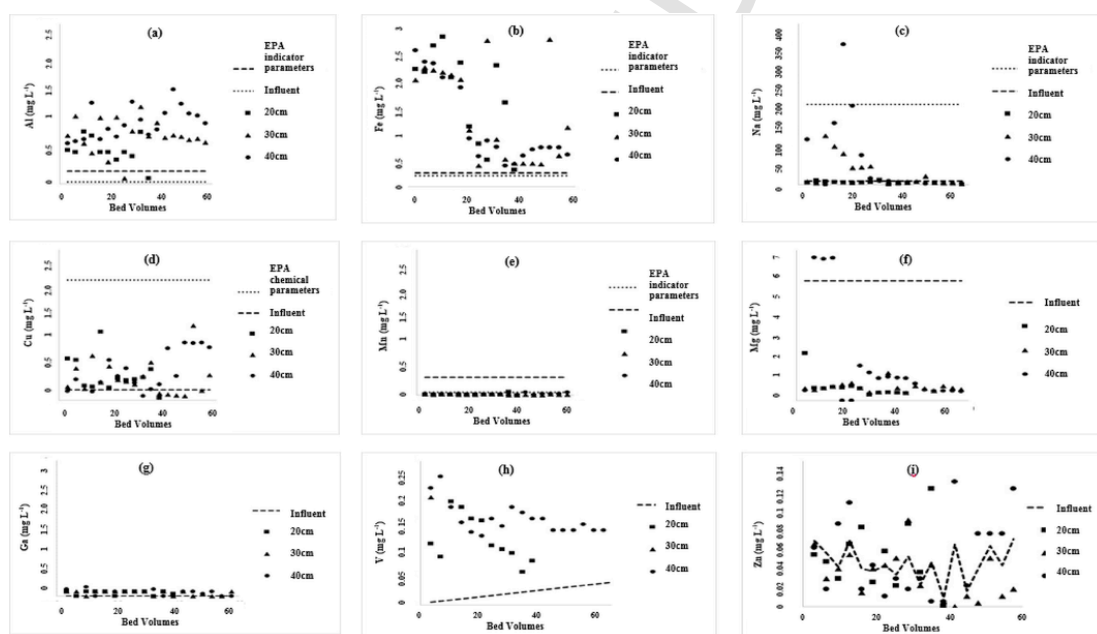


Fig. 7. Comparison of the composition of (a) Al, (b) Fe, (c) Na (d) Cu (e) Mn (f) Mg (g) Ga (h) V and (i) Zn in both the influent and effluent in the columns treating forest run-off over the 24–36h loading period. EPA indicator parameter or EPA chemical parameter included for each element.

position and concentration of elements in bauxite will vary depending on the type of ore (Mayes et al., 2011).

Although there was overall evidence of mobilisation of some trace elements while treating the wastewater, one suggestion would be to include a rinse/wash period prior to packing the columns. This would reduce and/or eliminate the potential leaching of metals at the initial loading period and avoid further release as the loading period increases. Another option would be to apply a seawater treatment to the bauxite residue, which has been proven to lower the pH and therefore reduce the leaching of metal(loid) species (Cusack et al., 2018; Johnston et al., 2010).

#### 4. Conclusions

Several studies have focussed on the use of low-cost adsorbents in the removal of contaminants such as P from contaminated waters due to possible cost savings and to reutilise by-products from various sectors. This study demonstrated that bauxite residue has P (particularly dissolved reactive phosphorus) removal capabilities in both low (forest run-off) and high (dairy soiled water) range P-concentrated waters. The estimated service time of the column media before initial breakthrough, based on the performance of the largest columns, was 1.08 min g<sup>-1</sup> media for the forest run-off and 0.28 min g<sup>-1</sup> media for the dairy soiled water. Due to the composition of the bauxite residue, potential for metal(loid) leaching is a concern. Aluminium and iron

were the dominant metals released in the treated effluent, but this may be eliminated by a preventative step such as introducing a washing period or a seawater neutralisation step prior to packing the bauxite residue into the columns.

## Acknowledgements

The authors would like to acknowledge the financial support of the Environmental Protection Agency (EPA) (2014-RE-MS-1).

## Appendix A. Supplementary data

Supplementary data to this article can be found online at <https://doi.org/10.1016/j.jenvman.2019.04.042>.

## Uncited Reference

European Drinking Water Directive (Council Directive 98/83/EC of 3 November 1998 on the quality of water intended for human consumption), 1998.

## References

- Acelas, N.Y., Martin, B.D., López, D., Jefferson, B., 2015. Selective removal of phosphate from wastewater using hydrated metal oxides dispersed within anionic exchange media. *Chemosphere* 119, 1353–1360. DOI Link: <https://doi.org/10.1016/j.chemosphere.2014.02.024>.
- Ádám, K., Sovik, A.K., Krogstad, T., Heistad, A., 2007. Phosphorus removal by the filter materials light-weight aggregates and shells and a review of processes and experimental set-ups for improved design of filter systems for wastewater treatment. *Vatten* 63 (3), 245.
- Akhurst, D.J., Jones, G.B., Clark, M., McConchie, D., 2006. Phosphate removal from aqueous solutions using neutralised bauxite refinery residues (Bauxsol™). *Environ. Chem.* 3 (1), 65–74. DOI Link: <https://doi.org/10.1071/EN05038>.
- Berzina-Cimdina, L., Borodajenko, N., 2012. Research of calcium phosphates using Fourier transform infrared spectroscopy. In: *Infrared Spectroscopy-Materials Science, Engineering and Technology*. InTech. Available [http://scholar.google.com/scholar\\_url?url=https%3A%2F%2Fwww.intechopen.com%2Fdownload%2Fpdf%2F36171&hl=en&sa=T&oi=ggp&ct=res&cd=0&d=1876013532413993455&ei=JQ5fW6ODB4SQmwHqQ7O4BA&scisig=AAGBfmOzcrG1iAsbV5fV1kKQs9aPk9QMNA&nossl=1&ws=1440x845](http://scholar.google.com/scholar_url?url=https%3A%2F%2Fwww.intechopen.com%2Fdownload%2Fpdf%2F36171&hl=en&sa=T&oi=ggp&ct=res&cd=0&d=1876013532413993455&ei=JQ5fW6ODB4SQmwHqQ7O4BA&scisig=AAGBfmOzcrG1iAsbV5fV1kKQs9aPk9QMNA&nossl=1&ws=1440x845), [accessed 30.07.2018].
- Bhatnagar, A., Vilar, V.J., Botelho, C.M., Boaventura, R.A., 2011. A review of the use of red mud as adsorbent for the removal of toxic pollutants from water and wastewater. *Environ. Technol.* 32 (3), 231–249. DOI Link: <https://doi.org/10.1080/09593330.2011.560615>.
- Bowden, L.L., Jarvis, A.P., Younger, P.L., Johnson, K.L., 2009. Phosphorus removal from waste waters using basic oxygen steel slag. *Environ. Sci. Technol.* 43 (7), 2476–2481.
- Brennan, R.B., Wall, D., Fenton, O., Grant, J., Sharpley, A.N., Healy, M.G., 2014. The impact of chemical amendment of dairy cattle slurry before land application on soil phosphorus dynamics. *Commun. Soil Sci. Plant Anal.* 45 (16), 2215–2233. DOI Link: <https://doi.org/10.1080/00103624.2014.912293>.
- Bridger, S., Knowles, M., 2000. A Complete Method for Environmental Samples by Simultaneous Axially Viewed ICP-AES Following USEPA Guidelines. *Varian ICP-OES at Work* (29), Available:[24.05.2018] <https://www.agilent.com/cs/library/applications/ICPES-29.pdf>.
- Burke, I.T., Mayes, W.M., Peacock, C.L., Brown, A.P., Jarvis, A.P., Gruiz, K., 2012. Speciation of arsenic, chromium, and vanadium in red mud samples from the Ajka spill site, Hungary. *Environ. Sci. Technol.* 46 (6), 3085–3092. <https://doi.org/10.1021/es3003475>.
- Burke, I.T., Peacock, C.L., Lockwood, C.L., Stewart, D.I., Mortimer, R.J., Ward, M.B., Renforth, P., Gruiz, K., Mayes, W.M., 2013. Behavior of aluminum, arsenic, and vanadium during the neutralization of red mud leachate by HCl, gypsum, or seawater. *Environ. Sci. Technol.* 47 (12), 6527–6535. <https://doi.org/10.1021/es4010834>.
- Callery, O., Brennan, R.B., Healy, M.G., 2015. Use of amendments in a peat soil to reduce phosphorus losses from forestry operations. *Ecol. Eng.* 85, 193–200 <https://doi.org/10.1016/j.ecoleng.2015.10.016>.
- Callery, O., Healy, M.G., Rognard, F., Barthelemy, L., Brennan, R.B., 2016. Evaluating the long-term performance of low-cost adsorbents using small-scale adsorption column experiments. *Water Res.* 101, 429–440 <https://doi.org/10.1016/j.watres.2016.05.093>.
- Callery, O., Healy, M.G., 2017. Predicting the propagation of concentration and saturation fronts in fixed-bed filters. *Water Res.* 123, 556–568 <https://doi.org/10.1016/j.watres.2017.07.010>.
- Castaldi, P., Silvetti, M., Enzo, S., Melis, P., 2010. Study of sorption processes and FT-IR analysis of arsenate sorbed onto red muds (a bauxite ore processing waste). *J. Hazard Mater.* 175 (1–3), 172–178 <https://doi.org/10.1016/j.jhazmat.2009.09.145>.
- Castaldi, P., Silvetti, M., Enzo, S., Deiana, S., 2011. X-ray diffraction and thermal analysis of bauxite ore-processing waste (red mud) exchanged with arsenate and phosphate. *Clay Clay Miner.* 59 (2), 189–199 <https://doi.org/10.1346/CCMN.2011.0590207>.
- Chen, J.P., Yoon, J.T., Yiacoumi, S., 2003. Effects of chemical and physical properties of influent on copper sorption onto activated carbon fixed-bed columns. *Carbon* 41 (8), 1635–1644 [https://doi.org/10.1016/S0008-6223\(03\)00117-9](https://doi.org/10.1016/S0008-6223(03)00117-9).
- Chen, N., Feng, C., Zhang, Z., Liu, R., Gao, Y., Li, M., Sugiura, N., 2012. Preparation and characterization of lanthanum (III) loaded granular ceramic for phosphorus and ammonium removal. *J. Environ. Sci.* 33 (1), 105–112 <https://doi.org/10.1016/j.jes.2011.11.018>.
- Chen, N., Feng, C., Zhang, Z., Liu, R., Gao, Y., Li, M., Sugiura, N., 2012. Preparation and characterization of lanthanum (III) loaded granular ceramic for phosphorus and ammonium removal. *J. Environ. Sci.* 33 (1), 105–112 <https://doi.org/10.1016/j.jes.2011.11.018>.
- Chen, N., Feng, C., Zhang, Z., Liu, R., Gao, Y., Li, M., Sugiura, N., 2012. Preparation and characterization of lanthanum (III) loaded granular ceramic for phosphorus and ammonium removal. *J. Environ. Sci.* 33 (1), 105–112 <https://doi.org/10.1016/j.jes.2011.11.018>.
- Chen, N., Feng, C., Zhang, Z., Liu, R., Gao, Y., Li, M., Sugiura, N., 2012. Preparation and characterization of lanthanum (III) loaded granular ceramic for phosphorus and ammonium removal. *J. Environ. Sci.* 33 (1), 105–112 <https://doi.org/10.1016/j.jes.2011.11.018>.
- Chen, N., Feng, C., Zhang, Z., Liu, R., Gao, Y., Li, M., Sugiura, N., 2012. Preparation and characterization of lanthanum (III) loaded granular ceramic for phosphorus and ammonium removal. *J. Environ. Sci.* 33 (1), 105–112 <https://doi.org/10.1016/j.jes.2011.11.018>.
- Chen, N., Feng, C., Zhang, Z., Liu, R., Gao, Y., Li, M., Sugiura, N., 2012. Preparation and characterization of lanthanum (III) loaded granular ceramic for phosphorus and ammonium removal. *J. Environ. Sci.* 33 (1), 105–112 <https://doi.org/10.1016/j.jes.2011.11.018>.
- Chen, N., Feng, C., Zhang, Z., Liu, R., Gao, Y., Li, M., Sugiura, N., 2012. Preparation and characterization of lanthanum (III) loaded granular ceramic for phosphorus and ammonium removal. *J. Environ. Sci.* 33 (1), 105–112 <https://doi.org/10.1016/j.jes.2011.11.018>.
- Chen, N., Feng, C., Zhang, Z., Liu, R., Gao, Y., Li, M., Sugiura, N., 2012. Preparation and characterization of lanthanum (III) loaded granular ceramic for phosphorus and ammonium removal. *J. Environ. Sci.* 33 (1), 105–112 <https://doi.org/10.1016/j.jes.2011.11.018>.
- Chen, N., Feng, C., Zhang, Z., Liu, R., Gao, Y., Li, M., Sugiura, N., 2012. Preparation and characterization of lanthanum (III) loaded granular ceramic for phosphorus and ammonium removal. *J. Environ. Sci.* 33 (1), 105–112 <https://doi.org/10.1016/j.jes.2011.11.018>.
- Chen, N., Feng, C., Zhang, Z., Liu, R., Gao, Y., Li, M., Sugiura, N., 2012. Preparation and characterization of lanthanum (III) loaded granular ceramic for phosphorus and ammonium removal. *J. Environ. Sci.* 33 (1), 105–112 <https://doi.org/10.1016/j.jes.2011.11.018>.
- Chen, N., Feng, C., Zhang, Z., Liu, R., Gao, Y., Li, M., Sugiura, N., 2012. Preparation and characterization of lanthanum (III) loaded granular ceramic for phosphorus and ammonium removal. *J. Environ. Sci.* 33 (1), 105–112 <https://doi.org/10.1016/j.jes.2011.11.018>.
- Chen, N., Feng, C., Zhang, Z., Liu, R., Gao, Y., Li, M., Sugiura, N., 2012. Preparation and characterization of lanthanum (III) loaded granular ceramic for phosphorus and ammonium removal. *J. Environ. Sci.* 33 (1), 105–112 <https://doi.org/10.1016/j.jes.2011.11.018>.
- Chen, N., Feng, C., Zhang, Z., Liu, R., Gao, Y., Li, M., Sugiura, N., 2012. Preparation and characterization of lanthanum (III) loaded granular ceramic for phosphorus and ammonium removal. *J. Environ. Sci.* 33 (1), 105–112 <https://doi.org/10.1016/j.jes.2011.11.018>.
- Chen, N., Feng, C., Zhang, Z., Liu, R., Gao, Y., Li, M., Sugiura, N., 2012. Preparation and characterization of lanthanum (III) loaded granular ceramic for phosphorus and ammonium removal. *J. Environ. Sci.* 33 (1), 105–112 <https://doi.org/10.1016/j.jes.2011.11.018>.
- Chen, N., Feng, C., Zhang, Z., Liu, R., Gao, Y., Li, M., Sugiura, N., 2012. Preparation and characterization of lanthanum (III) loaded granular ceramic for phosphorus and ammonium removal. *J. Environ. Sci.* 33 (1), 105–112 <https://doi.org/10.1016/j.jes.2011.11.018>.
- Chen, N., Feng, C., Zhang, Z., Liu, R., Gao, Y., Li, M., Sugiura, N., 2012. Preparation and characterization of lanthanum (III) loaded granular ceramic for phosphorus and ammonium removal. *J. Environ. Sci.* 33 (1), 105–112 <https://doi.org/10.1016/j.jes.2011.11.018>.
- Chen, N., Feng, C., Zhang, Z., Liu, R., Gao, Y., Li, M., Sugiura, N., 2012. Preparation and characterization of lanthanum (III) loaded granular ceramic for phosphorus and ammonium removal. *J. Environ. Sci.* 33 (1), 105–112 <https://doi.org/10.1016/j.jes.2011.11.018>.
- Chen, N., Feng, C., Zhang, Z., Liu, R., Gao, Y., Li, M., Sugiura, N., 2012. Preparation and characterization of lanthanum (III) loaded granular ceramic for phosphorus and ammonium removal. *J. Environ. Sci.* 33 (1), 105–112 <https://doi.org/10.1016/j.jes.2011.11.018>.
- Chen, N., Feng, C., Zhang, Z., Liu, R., Gao, Y., Li, M., Sugiura, N., 2012. Preparation and characterization of lanthanum (III) loaded granular ceramic for phosphorus and ammonium removal. *J. Environ. Sci.* 33 (1), 105–112 <https://doi.org/10.1016/j.jes.2011.11.018>.
- Chen, N., Feng, C., Zhang, Z., Liu, R., Gao, Y., Li, M., Sugiura, N., 2012. Preparation and characterization of lanthanum (III) loaded granular ceramic for phosphorus and ammonium removal. *J. Environ. Sci.* 33 (1), 105–112 <https://doi.org/10.1016/j.jes.2011.11.018>.
- Chen, N., Feng, C., Zhang, Z., Liu, R., Gao, Y., Li, M., Sugiura, N., 2012. Preparation and characterization of lanthanum (III) loaded granular ceramic for phosphorus and ammonium removal. *J. Environ. Sci.* 33 (1), 105–112 <https://doi.org/10.1016/j.jes.2011.11.018>.
- Chen, N., Feng, C., Zhang, Z., Liu, R., Gao, Y., Li, M., Sugiura, N., 2012. Preparation and characterization of lanthanum (III) loaded granular ceramic for phosphorus and ammonium removal. *J. Environ. Sci.* 33 (1), 105–112 <https://doi.org/10.1016/j.jes.2011.11.018>.
- Chen, N., Feng, C., Zhang, Z., Liu, R., Gao, Y., Li, M., Sugiura, N., 2012. Preparation and characterization of lanthanum (III) loaded granular ceramic for phosphorus and ammonium removal. *J. Environ. Sci.* 33 (1), 105–112 <https://doi.org/10.1016/j.jes.2011.11.018>.
- Chen, N., Feng, C., Zhang, Z., Liu, R., Gao, Y., Li, M., Sugiura, N., 2012. Preparation and characterization of lanthanum (III) loaded granular ceramic for phosphorus and ammonium removal. *J. Environ. Sci.* 33 (1), 105–112 <https://doi.org/10.1016/j.jes.2011.11.018>.
- Chen, N., Feng, C., Zhang, Z., Liu, R., Gao, Y., Li, M., Sugiura, N., 2012. Preparation and characterization of lanthanum (III) loaded granular ceramic for phosphorus and ammonium removal. *J. Environ. Sci.* 33 (1), 105–112 <https://doi.org/10.1016/j.jes.2011.11.018>.
- Chen, N., Feng, C., Zhang, Z., Liu, R., Gao, Y., Li, M., Sugiura, N., 2012. Preparation and characterization of lanthanum (III) loaded granular ceramic for phosphorus and ammonium removal. *J. Environ. Sci.* 33 (1), 105–112 <https://doi.org/10.1016/j.jes.2011.11.018>.
- Chen, N., Feng, C., Zhang, Z., Liu, R., Gao, Y., Li, M., Sugiura, N., 2012. Preparation and characterization of lanthanum (III) loaded granular ceramic for phosphorus and ammonium removal. *J. Environ. Sci.* 33 (1), 105–112 <https://doi.org/10.1016/j.jes.2011.11.018>.
- Chen, N., Feng, C., Zhang, Z., Liu, R., Gao, Y., Li, M., Sugiura, N., 2012. Preparation and characterization of lanthanum (III) loaded granular ceramic for phosphorus and ammonium removal. *J. Environ. Sci.* 33 (1), 105–112 <https://doi.org/10.1016/j.jes.2011.11.018>.
- Chen, N., Feng, C., Zhang, Z., Liu, R., Gao, Y., Li, M., Sugiura, N., 2012. Preparation and characterization of lanthanum (III) loaded granular ceramic for phosphorus and ammonium removal. *J. Environ. Sci.* 33 (1), 105–112 <https://doi.org/10.1016/j.jes.2011.11.018>.
- Chen, N., Feng, C., Zhang, Z., Liu, R., Gao, Y., Li, M., Sugiura, N., 2012. Preparation and characterization of lanthanum (III) loaded granular ceramic for phosphorus and ammonium removal. *J. Environ. Sci.* 33 (1), 105–112 <https://doi.org/10.1016/j.jes.2011.11.018>.
- Chen, N., Feng, C., Zhang, Z., Liu, R., Gao, Y., Li, M., Sugiura, N., 2012. Preparation and characterization of lanthanum (III) loaded granular ceramic for phosphorus and ammonium removal. *J. Environ. Sci.* 33 (1), 105–112 <https://doi.org/10.1016/j.jes.2011.11.018>.
- Chen, N., Feng, C., Zhang, Z., Liu, R., Gao, Y., Li, M., Sugiura, N., 2012. Preparation and characterization of lanthanum (III) loaded granular ceramic for phosphorus and ammonium removal. *J. Environ. Sci.* 33 (1), 105–112 <https://doi.org/10.1016/j.jes.2011.11.018>.
- Chen, N., Feng, C., Zhang, Z., Liu, R., Gao, Y., Li, M., Sugiura, N., 2012. Preparation and characterization of lanthanum (III) loaded granular ceramic for phosphorus and ammonium removal. *J. Environ. Sci.* 33 (1), 105–112 <https://doi.org/10.1016/j.jes.2011.11.018>.
- Chen, N., Feng, C., Zhang, Z., Liu, R., Gao, Y., Li, M., Sugiura, N., 2012. Preparation and characterization of lanthanum (III) loaded granular ceramic for phosphorus and ammonium removal. *J. Environ. Sci.* 33 (1), 105–112 <https://doi.org/10.1016/j.jes.2011.11.018>.
- Chen, N., Feng, C., Zhang, Z., Liu, R., Gao, Y., Li, M., Sugiura, N., 2012. Preparation and characterization of lanthanum (III) loaded granular ceramic for phosphorus and ammonium removal. *J. Environ. Sci.* 33 (1), 105–112 <https://doi.org/10.1016/j.jes.2011.11.018>.
- Chen, N., Feng, C., Zhang, Z., Liu, R., Gao, Y., Li, M., Sugiura, N., 2012. Preparation and characterization of lanthanum (III) loaded granular ceramic for phosphorus and ammonium removal. *J. Environ. Sci.* 33 (1), 105–112 <https://doi.org/10.1016/j.jes.2011.11.018>.
- Chen, N., Feng, C., Zhang, Z., Liu, R., Gao, Y., Li, M., Sugiura, N., 2012. Preparation and characterization of lanthanum (III) loaded granular ceramic for phosphorus and ammonium removal. *J. Environ. Sci.* 33 (1), 105–112 <https://doi.org/10.1016/j.jes.2011.11.018>.
- Chen, N., Feng, C., Zhang, Z., Liu, R., Gao, Y., Li, M., Sugiura, N., 2012. Preparation and characterization of lanthanum (III) loaded granular ceramic for phosphorus and ammonium removal. *J. Environ. Sci.* 33 (1), 105–112 <https://doi.org/10.1016/j.jes.2011.11.018>.
- Chen, N., Feng, C., Zhang, Z., Liu, R., Gao, Y., Li, M., Sugiura, N., 2012. Preparation and characterization of lanthanum (III) loaded granular ceramic for phosphorus and ammonium removal. *J. Environ. Sci.* 33 (1), 105–112 <https://doi.org/10.1016/j.jes.2011.11.018>.
- Chen, N., Feng, C., Zhang, Z., Liu, R., Gao, Y., Li, M., Sugiura, N., 2012. Preparation and characterization of lanthanum (III) loaded granular ceramic for phosphorus and ammonium removal. *J. Environ. Sci.* 33 (1), 105–112 <https://doi.org/10.1016/j.jes.2011.11.018>.
- Chen, N., Feng, C., Zhang, Z., Liu, R., Gao, Y., Li, M., Sugiura, N., 2012. Preparation and characterization of lanthanum (III) loaded granular ceramic for phosphorus and ammonium removal. *J. Environ. Sci.* 33 (1), 105–112 <https://doi.org/10.1016/j.jes.2011.11.018>.
- Chen, N., Feng, C., Zhang, Z., Liu, R., Gao, Y., Li, M., Sugiura, N., 2012. Preparation and characterization of lanthanum (III) loaded granular ceramic for phosphorus and ammonium removal. *J. Environ. Sci.* 33 (1), 105–112 <https://doi.org/10.1016/j.jes.2011.11.018>.
- Chen, N., Feng, C., Zhang, Z., Liu, R., Gao, Y., Li, M., Sugiura, N., 2012. Preparation and characterization of lanthanum (III) loaded granular ceramic for phosphorus and ammonium removal. *J. Environ. Sci.* 33 (1), 105–112 <https://doi.org/10.1016/j.jes.2011.11.018>.
- Chen, N., Feng, C., Zhang, Z., Liu, R., Gao, Y., Li, M., Sugiura, N., 2012. Preparation and characterization of lanthanum (III) loaded granular ceramic for phosphorus and ammonium removal. *J. Environ. Sci.* 33 (1), 105–112 <https://doi.org/10.1016/j.jes.2011.11.018>.
- Chen, N., Feng, C., Zhang, Z., Liu, R., Gao, Y., Li, M., Sugiura, N., 2012. Preparation and characterization of lanthanum (III) loaded granular ceramic for phosphorus and ammonium removal. *J. Environ. Sci.* 33 (1), 105–112 <https://doi.org/10.1016/j.jes.2011.11.018>.
- Chen, N., Feng, C., Zhang, Z., Liu, R., Gao, Y., Li, M., Sugiura, N., 2012. Preparation and characterization of lanthanum (III) loaded granular ceramic for phosphorus and ammonium removal. *J. Environ. Sci.* 33 (1), 105–112 <https://doi.org/10.1016/j.jes.2011.11.018>.
- Chen, N., Feng, C., Zhang, Z., Liu, R., Gao, Y., Li, M., Sugiura, N., 2012. Preparation and characterization of lanthanum (III) loaded granular ceramic for phosphorus and ammonium removal. *J. Environ. Sci.* 33 (1), 105–112 <https://doi.org/10.1016/j.jes.2011.11.018>.
- Chen, N., Feng, C., Zhang, Z., Liu, R., Gao, Y., Li, M., Sugiura, N., 2012. Preparation and characterization of lanthanum (III) loaded granular ceramic for phosphorus and ammonium removal. *J. Environ. Sci.* 33 (1), 105–112 <https://doi.org/10.1016/j.jes.2011.11.018>.
- Chen, N., Feng, C., Zhang, Z., Liu, R., Gao, Y., Li, M., Sugiura, N., 2012. Preparation and characterization of lanthanum (III) loaded granular ceramic for phosphorus and ammonium removal. *J. Environ. Sci.* 33 (1), 105–112 <https://doi.org/10.1016/j.jes.2011.11.018>.
- Chen, N., Feng, C., Zhang, Z., Liu, R., Gao, Y., Li, M., Sugiura, N., 2012. Preparation and characterization of lanthanum (III) loaded granular ceramic for phosphorus and ammonium removal. *J. Environ. Sci.* 33 (1), 105–112 <https://doi.org/10.1016/j.jes.2011.11.018>.
- Chen, N., Feng, C., Zhang, Z., Liu, R., Gao, Y., Li, M., Sugiura, N., 2012. Preparation and characterization of lanthanum (III) loaded granular ceramic for phosphorus and ammonium removal. *J. Environ. Sci.* 33 (1), 105–112 <https://doi.org/10.1016/j.jes.2011.11.018>.
- Chen, N., Feng, C., Zhang, Z., Liu, R., Gao, Y., Li, M., Sugiura, N., 2012. Preparation and characterization of lanthanum (III) loaded granular ceramic for phosphorus and ammonium removal. *J. Environ. Sci.* 33 (1), 105–112 <https://doi.org/10.1016/j.jes.2011.11.018>.
- Chen, N., Feng, C., Zhang, Z., Liu, R., Gao, Y., Li, M., Sugiura, N., 2012. Preparation and characterization of lanthanum (III) loaded granular ceramic for phosphorus and ammonium removal. *J. Environ. Sci.* 33 (1), 105–112 <https://doi.org/10.1016/j.jes.2011.11.018>.
- Chen, N., Feng, C., Zhang, Z., Liu, R., Gao, Y., Li, M., Sugiura, N., 2012. Preparation and characterization of lanthanum (III) loaded granular ceramic for phosphorus and ammonium removal. *J. Environ. Sci.* 33 (1), 105–112 <https://doi.org/10.1016/j.jes.2011.11.018>.
- Chen, N., Feng, C., Zhang, Z., Liu, R., Gao, Y., Li, M., Sugiura, N., 2012. Preparation and characterization of lanthanum (III) loaded granular ceramic for phosphorus and ammonium removal. *J. Environ. Sci.* 33 (1), 105–112 <https://doi.org/10.1016/j.jes.2011.11.018>.
- Chen, N., Feng, C., Zhang, Z., Liu, R., Gao, Y., Li, M., Sugiura, N., 2012. Preparation and characterization of lanthanum (III) loaded granular ceramic for phosphorus and ammonium removal. *J. Environ. Sci.* 33 (1), 105–112 <https://doi.org/10.1016/j.jes.2011.11.018>.
- Chen, N., Feng, C., Zhang, Z., Liu, R., Gao, Y., Li, M., Sugiura, N., 2012. Preparation and characterization of lanthanum (III) loaded granular ceramic for phosphorus and ammonium removal. *J. Environ. Sci.* 33 (1), 105–112 <https://doi.org/10.1016/j.jes.2011.11.018>.
- Chen, N., Feng, C., Zhang, Z., Liu, R., Gao, Y., Li, M., Sugiura, N., 2012. Preparation and characterization of lanthanum (III) loaded granular ceramic for phosphorus and ammonium removal. *J. Environ. Sci.* 33 (1), 105–112 <https://doi.org/10.1016/j.jes.2011.11.018>.
- Chen, N., Feng, C., Zhang, Z., Liu, R., Gao, Y., Li, M., Sugiura, N., 2012. Preparation and characterization of lanthanum (III) loaded granular ceramic for phosphorus and ammonium removal. *J. Environ. Sci.* 33 (1), 105–112 <https://doi.org/10.1016/j.jes.2011.11.018>.
- Chen, N., Feng, C., Zhang, Z., Liu, R., Gao, Y., Li, M., Sugiura, N., 2012. Preparation and characterization of lanthanum (III) loaded granular ceramic for phosphorus and ammonium removal. *J. Environ. Sci.* 33 (1), 105–112 <https://doi.org/10.1016/j.jes.2011.11.018>.
- Chen, N., Feng, C., Zhang, Z., Liu, R., Gao, Y., Li, M., Sugiura, N., 2012. Preparation and characterization of lanthanum (III) loaded granular ceramic for phosphorus and ammonium removal. *J. Environ. Sci.* 33 (1), 105–112 <https://doi.org/10.1016/j.jes.2011.11.018>.
- Chen, N., Feng, C., Zhang, Z., Liu, R., Gao, Y., Li, M., Sugiura, N., 2012. Preparation and characterization of lanthanum (III) loaded granular ceramic for phosphorus and ammonium removal. *J. Environ. Sci.* 33 (1), 105–112 [https://doi.org/10.1016/j.j](https://doi.org/10.1016/j.jes.2011.11.018)

- and limitations. *Waste Manag. Res.* 33 (7), 612–629 <https://doi.org/10.1177/0734242X15584841>.
- Johnston, M., Clark, M.W., McMahon, P., Ward, N., 2010. Alkalinity conversion of bauxite refinery residues by neutralization. *J. Hazard Mater.* 182 (1–3), 710–715 <https://doi.org/10.1016/j.jhazmat.2010.06.091>.
- Karageorgiou, K., Paschalis, M., Anastassakis, G.N., 2007. Removal of phosphate species from solution by adsorption onto calcite used as natural adsorbent. *J. Hazard Mater.* 139 (3), 447–452 <https://doi.org/10.1016/j.jhazmat.2006.02.038>.
- Kong, X., Li, M., Xue, S., Hartley, W., Chen, C., Wu, C., Li, X., Li, Y., 2017. Acid transformation of bauxite residue: conversion of its alkaline characteristics. *J. Hazard Mater.* 324, 382–390 <https://doi.org/10.1016/j.jhazmat.2016.10.073>.
- Lalley, J., Han, C., Mohan, G.R., Dionysiou, D.D., Speth, T.F., Garland, J., Nadagouda, M.N., 2015. Phosphate removal using modified Bayoxide® E33 adsorption media. *Environ. Sci. Water Res. Technol.* 1 (1), 96–107 <https://doi.org/10.1039/C4EW00020J>.
- Liu, Y., Lin, C., Wu, Y., 2007. Characterization of red mud derived from a combined Bayer Process and bauxite calcination method. *J. Hazard Mater.* 146, 255–261 <https://doi.org/10.1016/j.jhazmat.2006.12.015>.
- Loganathan, P., Vigneswaran, S., Kandasamy, J., Bolan, N.S., 2014. Removal and recovery of phosphate from water using sorption. *Crit. Rev. Environ. Sci. Technol.* 44 (8), 847–907.
- Lopez, E., Soto, B., Arias, M., Nunez, A., Rubinos, D., Barral, M.T., 1998. Adsorbent properties of red mud and its use for wastewater treatment. *Water Res.* 32, 1314–1322 [https://doi.org/10.1016/S0043-1354\(97\)00326-6](https://doi.org/10.1016/S0043-1354(97)00326-6).
- Mayes, W.M., Jarvis, A.P., Burke, I.T., Walton, M., Feigl, V., Klebercz, O., Gruiz, K., 2011. Dispersal and attenuation of trace contaminants downstream of the Ajka bauxite residue (red mud) depository failure, Hungary. *Environ. Sci. Technol.* 45 (12), 5147–5155 <https://doi.org/10.1021/es200850y>.
- Mayes, W.M., Burke, I.T., Gomes, H.I., Anton, Á.D., Molnár, M., Feigl, V., Ujaczki, J., 2016. Advances in understanding environmental risks of red mud after the Ajka spill, Hungary. *J. Sustain. Metall.* 2 (4), 332–343 <https://doi.org/10.1007/s40831-016-0050-z>.
- McConchie, D., Clark, M., Davies-McConchie, F., 2001. Processes and Compositions for Water Treatment. Neauveau Technology Investments, Australian, 28.
- Minogue, D., French, P., Bolger, T., Murphy, P.N.C., 2015. Characterisation of dairy soiled water in a survey of 60 Irish dairy farms. *Ir. J. Agric. Food Res.* 54 (1), 1–16 <https://doi.org/10.1515/ijaf-2015-0001>.
- Murnane, J.G., Brennan, R.B., Fenton, O., Healy, M.G., 2016. Zeolite combined with alum and aluminium chloride mixed with agricultural slurries reduces carbon losses in runoff from grassed soil boxes. *J. Environ. Qual.* 44 (5), 1674–1683 <https://doi.org/10.2134/jeq2016.05.0175>.
- Nowak, B., Aschenbrenner, P., Winter, F., 2013. Heavy metal removal from sewage sludge ash waste fly ash—a comparison. *Fuel Process. Technol.* 105, 195–201 <https://doi.org/10.1016/j.fuproc.2011.06.027>.
- O'Flynn, C.J., Fenton, O., Wall, D., Brennan, R.B., McLaughlin, M.J., Healy, M.G., 2018. Influence of soil phosphorus status, texture, pH and metal content on the efficacy of amendments to pig slurry in reducing phosphorus losses. *Soil Use Manag.* 34 (1), 1–8 <https://doi.org/10.1111/sum.12391>.
- Olszewska, J.P., Heal, K.V., Winfield, I.J., Eades, L.J., Spears, B.M., 2017. Assessing the role of bed sediments in the persistence of red mud pollution in a shallow lake (Kinghorn Loch, UK). *Water Res.* 123, 569–577 <https://doi.org/10.1016/j.watres.2017.07.009>.
- Pan, G., Lyu, T., Mortimer, R., 2018. Comment: Closing Phosphorus Cycle from Natural Waters: Re-capturing Phosphorus through an Integrated Water-Energy-Food Strategy. <https://doi.org/10.1016/j.jes.2018.02.018>.
- Penn, C., McGrath, J., Bowen, J., Wilson, S., 2014. Phosphorus removal structures: a management option for legacy phosphorus. *J. Soil Water Conserv.* 69 (2), 51A–56A <https://doi.org/10.2489/jswc.69.2.51A>.
- Pratt, C., Parsons, S.A., Soares, A., Martin, B.D., 2012. Biologically and chemically mediated adsorption and precipitation of phosphorus from wastewater. *Curr. Opin. Biotechnol.* 23 (6), 890–896 <https://doi.org/10.1016/j.copbio.2012.07.003>.
- Pretty, J., Bharucha, Z.P., 2014. Sustainable intensification in agricultural systems. *Ann. Bot.* 114 (8), 1571–1596 <https://doi.org/10.1093/aob/mcu205>.
- Ruane, E.M., Murphy, P.N., Healy, M.G., French, P., Rodgers, M., 2011. On-farm treatment of dairy soiled water using aerobic woodchip filters. *Water Res.* 45 (20), 6668–6676 <https://doi.org/10.1016/j.watres.2011.09.055>.
- Sharpley, A., 2016. Managing agricultural phosphorus to minimize water quality impacts. *Sci. Agric.* 73 (1), 1–8 <https://doi.org/10.1590/0103-9016-2015-0107>.
- Søvik, A.K., Kløve, B., 2005. Phosphorus retention processes in shell sand filter systems treating municipal wastewater. *Ecol. Eng.* 25 (2), 168–182 <https://doi.org/10.1016/j.ecoleng.2005.04.007>.
- Stumm, W., 1992. Chemistry of the Solid-Water Interface: Processes at the Mineral-Water and Particle-Water Interface in Natural Systems. John Wiley & Son Inc.
- Sukačová, K., Trtřlek, M., Rataj, T., 2015. Phosphorus removal using a microalgal biofilm in a new biofilm photobioreactor for tertiary wastewater treatment. *Water Res.* 71, 55–63 <https://doi.org/10.1016/j.watres.2014.12.049>.
- Tejedor-Tejedor, M.I., Anderson, M.A., 1990. The protonation of phosphate on the surface of goethite as studied by CIR-FTIR and electrophoretic mobility. *Langmuir* 6 (3), 602–611 [http://doi.org/0743-7463/90/2406-0602\\$02.50/0](http://doi.org/0743-7463/90/2406-0602$02.50/0).
- Tresintsi, S., Simeonidis, K., Katsikini, M., Paloura, E.C., Bantsis, G., Mitrakas, M., 2014. A novel approach for arsenic adsorbents regeneration using MgO. *J. Hazard Mater.* 265, 217–225 <https://doi.org/10.1016/j.jhazmat.2013.12.003>.
- Ujaczki, J., Feigl, V., Molnár, M., Cusack, P., Curtin, T., Courtney, R., O'Donoghue, L., Davris, P., Hugi, C., Evangelou, M.W., Balomenos, E., 2018. Re-using bauxite residues: benefits beyond (critical raw) material recovery. *J. Chem. Technol. Biotechnol.* 93 (9), 2498–2510 <https://doi.org/10.1002/jctb.5687>.
- United Nations, 2015. Transforming Our World: the 2030 Agenda for Sustainable Development, Available [http://www.un.org/en/development/desa/population/migration/generalassembly/docs/globalcompact/A\\_RES\\_70\\_1\\_E.pdf](http://www.un.org/en/development/desa/population/migration/generalassembly/docs/globalcompact/A_RES_70_1_E.pdf) Accessed 18 July 2018.
- Vuković, G.D., Marinković, A.D., Škapin, S.D., Ristić, A., Aleksić, R., Perić-Grujić, A.A., Uskoković, P.S., 2011. Removal of lead from water by amino modified multi-walled carbon nanotubes. *Chem. Eng. J.* 173 (3), 855–865 <https://doi.org/10.1016/j.cej.2011.08.036>.
- Wang, B., Lehmann, J., Hanley, K., Hestrin, R., Enders, A., 2015. Adsorption and desorption of ammonium by maple wood biochar as a function of oxidation and pH. *Chemosphere* 138, 120–126 <https://doi.org/10.1016/j.chemosphere.2015.05.062>.
- Wang, X.X., Wu, Y.H., Zhang, T.Y., Xu, X.Q., Dao, G.H., Hu, H.Y., 2016. Simultaneous nitrogen, phosphorous, and hardness removal from reverse osmosis concentrate by microalgae cultivation. *Water Res.* 94, 215–224 <https://doi.org/10.1016/j.watres.2016.02.062>.
- Weissert, C., Kehr, J., 2018. Macronutrient sensing and signaling in plants. In: *Plant Macronutrient Use Efficiency*. pp. 45–64 <https://doi.org/10.1016/B978-0-12-811308-0.00003-X>.
- Wu, K., Chen, Y., Ouyang, Y., Lei, H., Liu, T., 2018. Adsorptive removal of fluoride from water by granular zirconium–aluminum hybrid adsorbent: performance and mechanisms. *Environ. Sci. Pollut. Res.* 25 (16), 15390–15403 <https://doi.org/10.1007/s11356-018-1711-1>.
- Ye, J., Zhang, P., Hoffmann, E., Zeng, G., Tang, Y., Dresely, J., Liu, Y., 2014. Comparison of response surface methodology and artificial neural network in optimization and prediction of acid activation of Bauxsol for phosphorus adsorption. *Water, Air, Soil Pollut.* 225 (12), 2225 <https://doi.org/10.1007/s11270-014-2225-1>.
- Zhou, Z., Hu, D., Ren, W., Zhao, Y., Jiang, L.M., Wang, L., 2015. Effect of humic substances on phosphorus removal by struvite precipitation. *Chemosphere* 141, 94–99 <https://doi.org/10.1016/j.chemosphere.2015.06.089>.
- Zhou, B., Xu, Y., Vogt, R.D., Lu, X., Li, X., Deng, X., Yue, A., Zhu, L., 2016. Effects of land use change on phosphorus levels in surface waters—a case study of a watershed strongly influenced by agriculture. *Water, Air, Soil Pollut.* 227 (5), 160 <https://doi.org/10.1007/s11270-016-2855-6>.
- Zhu, F., Li, Y., Xue, S., Hartley, W., Wu, H., 2016. Effects of iron-aluminium oxides and organic carbon on aggregate stability of bauxite residues. *Environ. Sci. Pollut. Res.* 23 (9), 9073–9081 <https://doi.org/10.1007/s11356-016-6172-9>.
- Zhu, X., Li, W., Zhang, Q., Zhang, C., Chen, L., 2018. Separation characteristics of vanadium from leach liquor of red mud by ion exchange with different resins. *Hydrometallurgy* 176, 42–48 <https://doi.org/10.1016/j.hydromet.2018.01.009>.